Atomistic simulation of hydrophobin HFBII conformation in aqueous and fluorous media and at the water/vacuum interface

Giuseppina Raffaini [a,b,*], Roberto Milani [c], Fabio Ganazzoli [a,b], Giuseppe Resnati [a,b,d], Pierangelo Metrangolo [a,b,c,d]

[a] Dipartimento di Chimica, Materiali ed Ingegneria Chimica "Giulio Natta", Politecnico di Milano, Via L. Mancinelli 7, 20131 Milano, Italy
[b] Unità Politecnico, INSTM, Piazza Leonardo da Vinci 32, 20133 Milano, Italy
[c] VTT Technical Research Centre of Finland Ltd., Biologinkuja 7, Espoo, Finland
[d] Laboratory of Nanostructured Fluorinated Materials (NFMLab), Dipartimento di Chimica, Materiali ed Ingegneria Chimica "Giulio Natta", Politecnico di Milano, Via L. Mancinelli 7, 20131 Milano, Italy

Hydrophobins are proteins of interest for numerous applications thanks to their unique conformational and surface properties and their ability to self-assemble at interfaces. Here we report fully atomistic molecular mechanics and molecular dynamics results together with circular dichroism experimental data, aimed to study the conformational properties of the hydrophobin HFBII in a fluorinated solvent in comparison with a water solution and/or at an aqueous/vacuum interface. Both the atomistic simulations and the circular dichroism data show the remarkable structural stability of HFBII at all scales in all these environments, with no significant structural change, although a small cavity is formed in the fluorinated solvent. The combination of theoretical calculations and circular dichroism data can describe in detail the protein conformation and flexibility in different solvents and/or at an interface, and constitutes a first step towards the study of their self-assembly.

Keywords: Hydrophobin, Protein conformation, Circular dichroism, Computer simulations, Molecular dynamics

1. Introduction

Hydrophobins are a family of small, film-forming proteins produced by filamentous fungi, endowed with exceptional surface activity features which make them effective coating or protective agents, adhesion promoters and surface modifiers [1–5]. Hydrophobins have possible interesting applications for instance in food technology [6,7], in the formation of biocompatible surfaces for biosensors [4], and in the surface modification of biomimetic composite materials [8,9]. It was recently shown that hydrophobins also effectively stabilize dispersions of fluorous materials in water by self-assembling at the interface [10–13]. Since protein surface activity and self-assembly at hydrophilic–hydrophobic interfaces is usually linked to denaturation of the individual molecules, in this work we study the stability of the hydrophobin HFBII in water, in a fluorinated solvent, and at the air/water interface, using Molecular Mechanics (MM) and Molecular Dynamics (MD) methods at a fully atomistic level, and adopting a simulation protocol formerly used by us [14–18] to model the conformational properties and stability of unlike proteins, in particular when adsorbed on solid biomaterial surfaces. The theoretical results will also be compared when possible with previous MD simulations, which used a coarse-grained model, yielding some chemical details for HFBI in water and at a water/octane interface [19], or a fully atomistic model in water and at a water/decane interface [20]. Furthermore, we report new circular dichroism (CD) data of HFBII in water and in an emulsion of a fluorinated solvent in order to compare these experimental data with the theoretical results.

Article history:
Received 14 September 2015
Received in revised form 5 October 2015
Accepted 6 November 2015
Available online 10 November 2015

* Corresponding author.
E-mail addresses: giuseppina.raffaini@polimi.it (G. Raffaini), roberto.milani@vtt.fi (R. Milani), pierangelo.metrangolo@polimi.it (P. Metrangolo).

2. Experimental methods

2.1. Materials

HFBII (molecular weight 7.5 kDa) was produced using recombinant strains of *Trichoderma reesei*, purifed by RP-HPLC as previously described [21] and freeze-dried before use. Galden® SV90 is a low molecular weight perfluoropolyether fluid (boiling point 90 °C) produced by Solvay Specialty Polymers, which was used without further purification.

Published Journal Article available at http://dx.doi.org/10.1016/j.jmgm.2015.11.006

2.2. Circular dichroism experiments

Circular dichroism experiments were performed on an Applied Photophysics Chirascan spectrometer. Solutions of HFBI in milli-Q water (100 μg/ml) were treated in a sonicator bath for 30 min at 40 °C, followed by mixing in a thermomixer at 25 °C (1000 rpm, 1 h). The emulsions were prepared by addition of 25 μl of Galden® SV90 to 475 μl of the HFBI solution (ratio 1:20) and ultrasonication of the mixture with an ultrasonic probe (Soniprep150 MSE, 26 mm tip, 750 W, 20 kHz, 30% amplitude 30%, 5 × 50 s). Analyses were performed on freshly prepared samples in a 0.1 cm path length quartz cuvette at 25 °C, scanning the λ = 180–260 nm region, with a step size of 0.5 nm, a minimum time/step of 3.0 s with adaptive evaluation option enabled, bandwidth 1 nm, 10 repetitions/sample. Spectra were averaged and smoothed.

2.3. Molecular mechanics and molecular dynamics methods

The simulation studies based on MM and MD methods were performed with InsightII/Discover 2000, Materials Studio and Discovery Studio [22] using the COMPASS force field. The coordinates of the non-hydrogen atoms of HFBII were taken from the X-ray structure [3] deposited within the Protein Data Bank (2B97), and the hydrogen atoms were added in the calculated position. Using the periodic boundary conditions the simulation box to study the HFBII protein in water was a cubic cell of size 50 Å (more than twice the protein size), and to model the water/*vacuum* interface we considered a cell with dimensions of 50 × 50× 120 Å adopting an NVT statistical ensemble. The protein in the fluorinated solvent (Galden®, modeled as CF_3-O-(CF_2-CF(CF_3)-O)$_n$-(CF_2-O)$_m$-CF_3 with n, m= 1, density equal to 1.69 g/cm^3) was modeled within a cubic cell of 50 Å using the *Amorphous Cell Tools* Modulus of Materials Studio. All energy minimizations were carried out up to an energy gradient lower than 4×10^{-3} kJ mol^{-1} Å^{-1}. The MD runs were performed at a constant T (300 K) controlled through the Berendsen thermostat. Integration of the dynamical equations was carried out with the Verlet algorithm using a time step of 1 fs, and the instantaneous coordinates were periodically saved for further analysis or geometry optimization. The length of the MD run was 60 ns in aqueous solution and 60 ns in the fluorinated solvent to check the system stability. The system equilibration on the time-scale of the present simulations was monitored through the time changes of the total and potential energy and of their components (the electrostatic and van der Waals contribution, as well as the intramolecular terms), and of the geometrical parameters such as the molecular size and radius of gyration, which showed in any case a stationary behavior for most of the latter part of the MD run.

In order to better describe the possible conformational changes of the HFBII protein, in particular the stability of its secondary structure in water, at the water/*vacuum* interface and in the fluorinated solvent, we used (i) the Ramachandran maps to monitor the changes in the (ψ,ϕ) torsion angles adjacent to the C_α atoms in the different environments, hence the conformational changes related to the protein secondary structure, and (ii) the root-mean-square distance (RMSD) maps [14–18] to determine the average distances of the same backbone atoms at different times within an MD trajectory at room temperature irrespective of its diffusional behavior. In particular, significant conformational changes in the secondary structure are shown by RMSD values of the order of 1 Å or more, whereas purely rigid-body diffusive (either translational or rotational) motion displays much smaller RMSD values, thus allowing to separate local from global motion. The RMSD map is constructed by calculating for a given set of n instantaneous conformations, or frames, the $n \times n$ root-mean-square distances among selected atoms (for instance the backbone atoms), and plotting them as a function of the frame indices as a bi-dimensional map with an appropriate color coding. The above-described RMSD between two frames is the minimum value of the function calculated with respect to the position of the centers of mass and the orientation of the principal axes of the molecule in the a and b frames

$$\left\{ \frac{1}{N} \sum_{i=1}^{N} \left(\boldsymbol{r}_i^a - \boldsymbol{r}_i^b \right)^2 \right\}^{1/2} \quad (1)$$

where the index i runs over the N selected atoms, the a, b superscripts indicate two different frames, and r is the vector position of the given atom, while the minimum value is chosen to remove trivial effects related to rigid-body translations or rotations of the whole system, thus getting rid of the above-mentioned diffusive motion. Therefore, similar conformations have a small RMSD, and unlike conformations a large RMSD.

Moreover, in order to describe the distribution of the solvent molecules around HFBII we used the Pair Distribution Function (PDF) [14–18], giving the probability density of finding a given set of atoms as a function of their distance r from another set within an MD run: for instance, in the case of solvation we considered the outer atoms of the solvent in the first set, and the protein atoms as the second set.

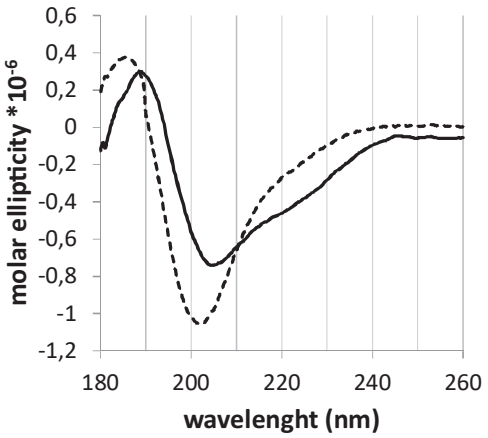

Fig. 1. Circular dichroism spectra of HFBII in water (dashed line) and in a 5% v/v emulsion of Galden® SV90 in water.

3. Results and discussion

CD spectroscopy was employed to experimentally investigate possible changes in the secondary structure of HFBII in fluorous/aqueous emulsions. To this end, we compared the CD spectrum of HFBII in water to that of a 5% v/v emulsion of the perfluoropolyether oil Galden® SV90 in aqueous HFBII solution (protein concentration: 0.1 mg/ml in both cases). Both spectra are reported in Fig. 1. It should be remarked here that the emulsions were stable for the entire timescale of the experiment, as confirmed by the absence of significant changes in the spectra obtained in subsequent measurement replicates on the same sample.

The negative band, originally centered around 202 nm in the HFBII spectrum in water, becomes clearly red-shifted to about 206 nm when analyzing fluorous oil-in-water emulsions. In addition, the onset of a broad negative shoulder is observed in the 225 nm area for the emulsified sample.

These changes are diagnostic of a small increase in the α-helical content within the protein structure, and suggest that the presence of the fluorinated solvent has some minor effect on it. Indeed, such observations appear to be consistent with those reported by Askolin et al. [23], who performed CD analysis on aqueous solutions of HFBII

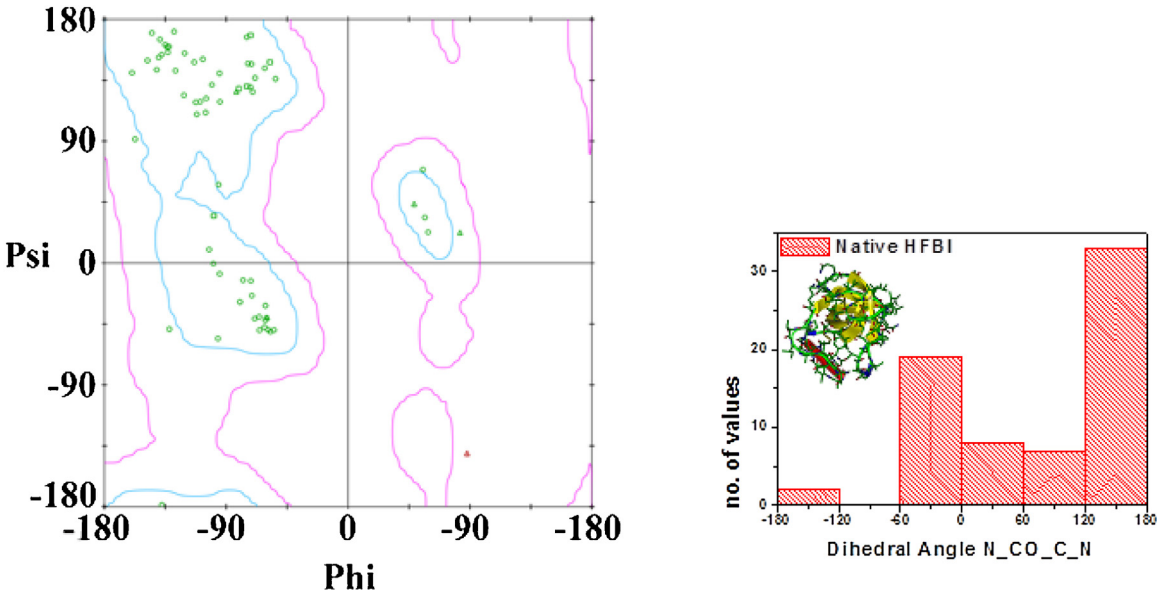

Fig. 2. The Ramachandran plot of the native HFBII (left) and the distribution of the ψ torsion angles of HFBII in the native state (right). The inset displays the secondary structure consisting of a α-helix (comprising 10 amino acids) in red, and β-sheets in yellow. The random-coil residues are shown in green, and the regular turns in blue. (For interpretation of the references to color in this figure legend, the reader is referred to the web version of this article.)

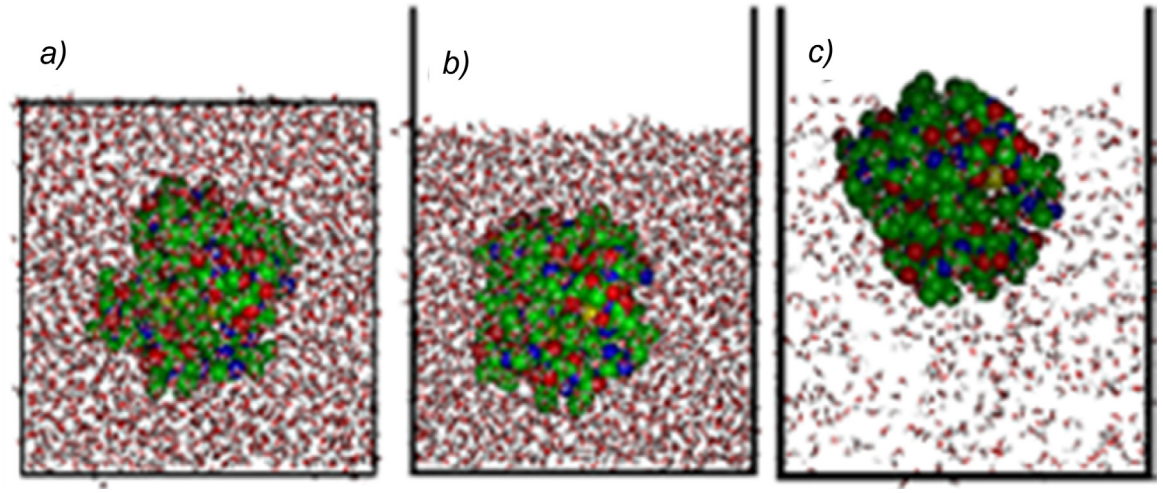

Fig. 3. (a) Initial optimized geometry of the simulation cubic cell containing HFBII, without hydrogen atoms for clarity, in water. (b) Initial optimized geometry of HFBII at the water/*vacuum* interface. (c) The geometry obtained starting from the system indicated in (b) after about 0.8 ns of the MD run at room temperature: the picture shows only the water molecules initially present in the simulation periodic cell that were still there at the end of the MD run, while the missing ones (see panel b) were replaced by their periodic images.

containing solid dispersed Teflon® particles. It seems therefore that HFBII assembles on the liquid fluorous droplets in much the same way as it does on solid fluorinated surfaces, at least as far as the protein structure is concerned.

Although some changes are observed, it appears that no extensive denaturation of the protein occurs, which testifies to the exceptional structural stability of hydrophobins due to the presence of four disulphide bridges in the protein core. The conclusions drawn from CD data, in particular about the structural stability of HFBII in strongly unlike environments, are fully consistent with theoretical results obtained by MD methods, reported below.

In order to describe at atomistic level the properties of HFBII, the conformational properties of the native HFBII protein as obtained by the high-resolution X-ray structure [3] were first studied through the Ramachandran plot (Fig. 2 at left). It should be remembered that these plots give a local picture of the protein conformation, and provide an immediate description of their secondary structure. Furthermore, these maps easily allow monitoring the conformational changes of a protein that may take place in different environments, due either to a specific solvent, as in the present case, or on a surface, for instance. Mapping the torsion angles (ϕ,ψ) along the backbone yielded, as expected, populated (ϕ,ψ) values typical of both α-helix and β-sheet structures. In this way, we can better quantitatively compare the conformational changes of HFBII in water or in a fluorinated solvent environment. In particular, since the ϕ values do only show relatively minor changes, we first report the distribution of the ψ angles of native HFBII in Fig. 2 (right panel), where the inset displays the protein secondary structure. Moreover, the protein surface area of the native HFBII, given by the surface accessible to a spherical probe with a radius of 1.4 Å (roughly the size of a water molecule), amounts to 3305 Å^2 (see Fig. S.1 in Supporting information). In the native state the HFBII radius of gyration is 10.76 Å and the intramolecular H-bonds are 52.

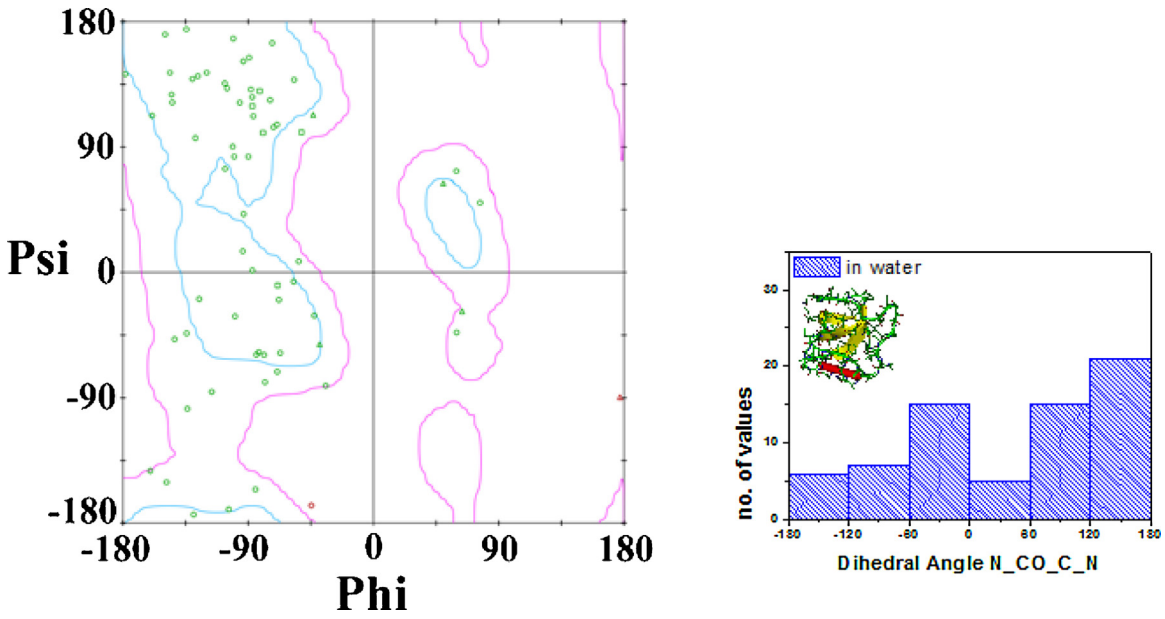

Fig. 4. The Ramachandran plot of HFBII in the initial optimized geometry in water considering a cubic simulation cell (size 50 Å). The corresponding distribution of the ψ angles of the HFBII backbone is shown on the right, where the inset shows the secondary structure of the optimized hydrated protein.

In order to study the hydration effects, as a second step, using the periodic boundary conditions we considered a single HFBII in a simulation box (a cubic cell with the size of 50 Å) with about 3800 water molecules (see Fig. 3a). Energy minimization of the initial geometry in water (Fig. 3a) shows that small conformational changes take place to better expose the hydrophilic residues forming hydrogen bonds with the water molecules. In fact, the protein envelope is rather similar to that found in the X-ray solid state structure, but the intramolecular H-bonds decrease to 48 due to formation of H-bonds with water, while the number of the amino acids in the α-helix does not change, and the β-sheets become marginally longer.

The Ramachandran plot of this conformation is shown in Fig. 4 (left panel). In the right panel of the same figure, the secondary structure and the distribution of the ψ angles in this initial geometry, optimized in water solution, are also reported: we notice that there is a significant decrease of the number of torsion angles close to 180°, compensated by an increase of those close to, but smaller than 120°. This implies that larger distortions from planarity are present in aqueous environment. On the other hand, in this optimized geometry the accessible surface area is equal to 3292 Å^2 (see Fig. S.2) and the radius of gyration is equal to 10.83 Å, with a hardly significant change from the native state.

After the MD run at room temperature lasting for 60 ns, no significant change in the protein envelope takes place, as also shown by the root-mean-square distance of the HFBII backbone atoms (the RMSD defined in Section 2). In particular, only in the very initial part of the MD run some minor conformational changes take place, with RMSD values of about 1 Å mainly involving small rearrangements in particular of some random sequences in order to optimize all the hydrogen bonds with water. Afterwards, no other relevant rearrangement is found, as shown by the very small RMSD values always smaller than 0.33 Å, which confirm the structural stability of the protein (the compete RMSD map obtained for the whole dynamic trajectory in water is shown in Fig. S.3). The distribution of the water molecules around HFBII is best described through the Pair Distribution Function (PDF, see Section 2) of the oxygen and hydrogen atoms of water molecules calculated from the MD trajectory as a function of their distance from the HFBII atoms. The PDF reported in Fig. 5 shows that they lie at the typical distances of H-bonds. There is some indication of additional, ordered solvent shells

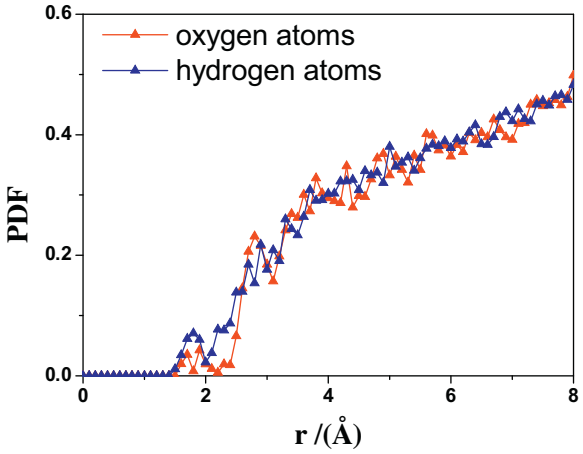

Fig. 5. PDF of oxygen (in red) and hydrogen atoms (in blue) around the HFBII calculated during the MD run in water. (For interpretation of the references to color in this figure legend, the reader is referred to the web version of this article.)

close to the HFBII surface, in particular for the second and possibly the third peak in the curve for the water oxygens; this distribution is similar to that found in a previous study about water molecules distribution around proteins in aqueous solution [14–18].

As a third step in studying the conformational properties of HFBII at the water/*vacuum* interface, a much larger cell was then adopted by increasing the *c* cell axis to 120 Å and including a *vacuum* space in the upper part to model a water-air interface, as reported in Fig. 3b. After the initial optimization, and in keeping with expectations, we found that during the MD run at room temperature the HFBII protein migrates to the interface within 1 ns (see the animation in S.4a). It is important to point out for the later discussion that in this way the residues belonging to the protein's hydrophobic patch, such as some topologically distant leucines and isoleucines, for example Leu7, Leu63, and Val18-Leu19-Asp20-Leu21-Ile22 are exposed to *vacuum* in order to avoid interaction with water (see Fig. 6 with the labeled amino acids and the secondary structure). Interestingly, and not unexpectedly, a similar

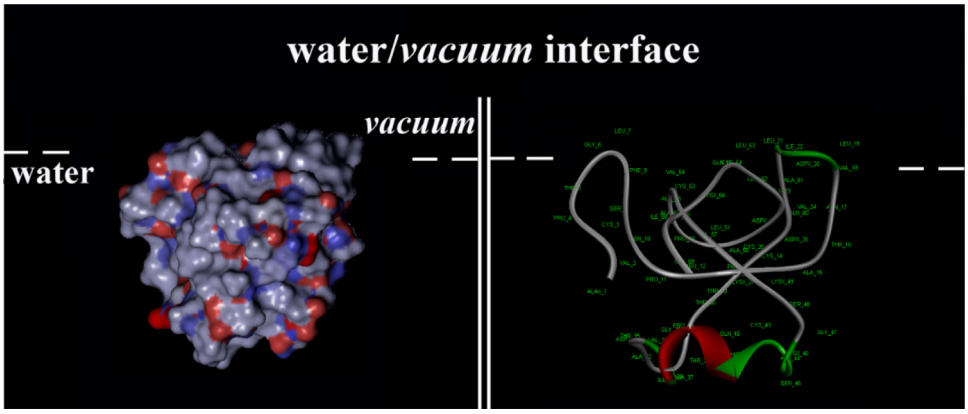

Fig. 6. The HFBII protein after reaching the water/*vacuum* interface: the figure shows the surface accessible to the solvent (left), and the secondary structure with the labeled aminoacids (right).

result was also obtained by fully atomistic simulations of HFBI at the water/*vacuum* interface [20].

It should be pointed out that during the MD run, the diffusing protein maintains its overall and local structure, and does not show any significant change in its overall shape compared to what was found after the initial optimization in water. In fact, the RMSD values of the backbone atoms (see Fig. S.4b) are in the range (0–0.33) Å, indicating a remarkable structural stability with minor conformational changes of the secondary structure. In particular, we find some lengthening of the α-helix which furthermore becomes a bit looser, and a partial loss of the β-sheet structure, in particular close to the interface (see Fig. 6).

While previously reported CD experiments did not show any significant change in secondary structure at the air/water interface compared to water [5], it must be pointed out that the protein self-assembly in the former environment prevents any detailed comparison with the present simulation results. Similar theoretical results with a coarse-grained model [19] of the analogous hydrophobin HFBI in water/octane, or an atomistic model at a water/*vacuum* or water/decane interface [20] were found concerning both the migration to the interface and the protein structural stability.

Finally, we simulated the conformational properties of HFBII in a fluorinated phase, modeling a perfluoropolyether solvent (see Fig. S.5) having a chemical structure analogous to that of Galden®, CF_3-O-(CF_2-$CF(CF_3)$-O)$_n$-(CF_2-O)$_m$-CF_3 ($n, m = 1$), using the periodic boundary conditions in a cubic cell with a size of 50 Å and containing 291 solvent molecules (6693 atoms). While HFBII is not soluble in Galden®, it is reasonable to assume that the hydrophobic patch of the protein will be embedded in the hydrophobic phase in a fluorous/aqueous biphasic system [22]. Therefore, the results of this simulation are expected to be particularly valuable as a first approach to study the conformation of the residues belonging to the hydrophobic patch in such systems. The Ramachandran plot of this conformation, giving a picture of the protein secondary structure, is reported in Fig. 6 (left panel), and the picture of the simulation cell is shown on the right panel of the same figure together with the distribution of the ψ torsional angles.

After the initial optimization of the HFBII protein in a fluorinated solvent, the radius of gyration with respect to the native state increases to 11.30 Å, while the intramolecular H-bonds are 42, i.e. fewer than in the solid state and in water, and the accessible surface increases to 3980 Å^2. In the fluorinated solvent, the intramolecular changes lead to a minor decrease in the length of the α-helix by one residue and to some loosening at one end, together with a partial loss of the β-sheet structure mainly involving the hydrophilic residues. Moreover, according to the present simulations these intramolecular rearrangements lead also to the formation of a cavity through the protein, barely accessible to a spherical probe having the radius of 1.4 Å, clearly visible in Fig. 8.

It is important to note that this cavity involves the protein fragment Thr16-Ile22, containing four amino acids with hydrophobic side chains which belong to the protein's hydrophobic patch (see Fig. 8 with the labeled amino acids and the secondary structure). We stress that these amino acids were found to be exposed to *vacuum* in the simulation in water (see Fig. 6), and are expected to be embedded in the hydrophobic phase at a fluorous/aqueous interface [22]. It can be assumed for this protein fragment to acquire a more relaxed and slightly looser structure in the hydrophobic environment of the fluorinated solvent than in water, where a more compact conformation allows to minimize unfavorable interactions. As done before, we also report in Fig. 7 the distribution of the ψ dihedral angles, somehow describing the secondary structure of the protein: the above-mentioned slightly looser structure leads to a small increase of some of these values from the 60–120° to the 120–180° range. Such relatively small changes indicating a noticeable overall structural stability are consistent with the CD experimental results reported above and with the simulations of HFBII in octane and of HFBI in decane [19,20]. It is also interesting to remark that an analogous extended conformation has been observed in the crystal structure of the hydrophobin HFBI [5], which is known to have a very similar structure to HFBII [3]. In that case, the extended conformation was found in two of the four molecules of a protein tetramer and involved the Ala61-Ala67 β-hairpin, which contains three other amino acids belonging to the hydrophobic patch. This conformational change was proposed to be driven by the formation of the tetramer, which occurs by association of the hydrophobic patches of the monomers.

During the MD run, the protein does not show any significant conformational changes in its overall shape, as shown also in this case by the RMSD values of the backbone atoms (see Fig. S.6) falling again in the range (0–0.33) Å. Thus, also in a fluorinated solvent HFBII displays very minor conformational changes of the secondary structure and appears to be structurally very stable.

The distribution of solvent molecules around HFBII is described as done before through the PDF of the oxygen and fluorine atoms of the solvent as a function of their distance from the protein atoms, calculated from an MD run of 5 ns at room temperature. The results, reported in Fig. 9, indicate that the solvent can closely approach the protein, but not as much as in water due to the lack of intermolecular hydrogen bonds. This is consistent with the experimental observation that HFBII is essentially insoluble in Galden®. Moreover, the distribution of the solvent atoms around the protein increases more slowly with the distance and is less ordered than in

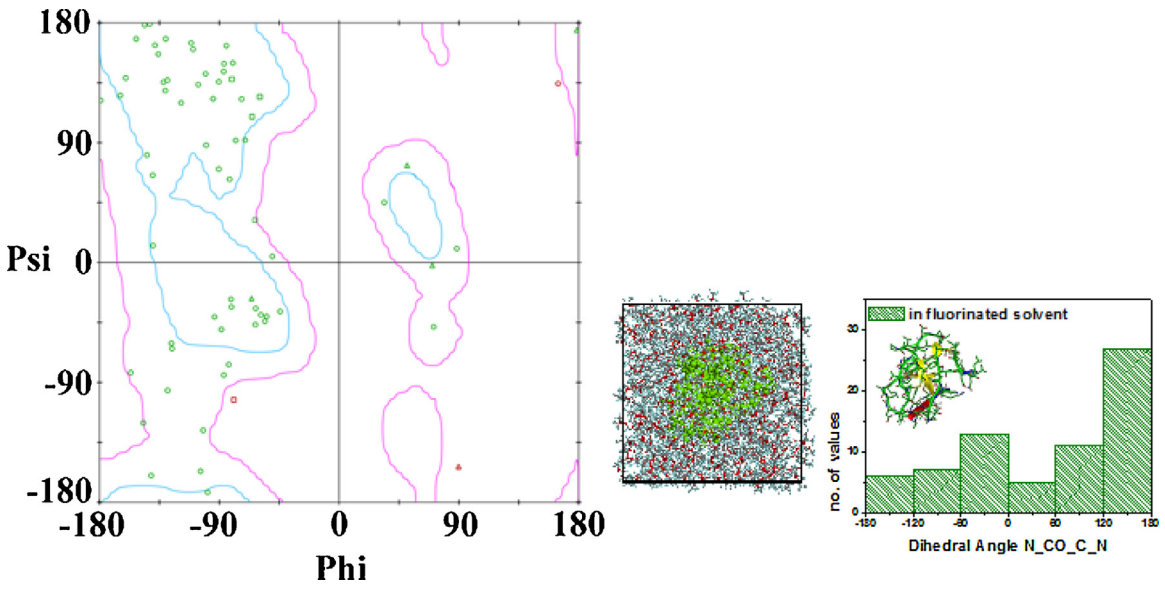

Fig. 7. The Ramachandran plot of HFBII in the fluorinated solvent (CF_3-O-(CF_2-$CF(CF_3)$-O)$_n$-(CF_2-O)$_m$-CF_3, n, $m = 1$) (left), and the HFBII protein (in green) in the fluorinated solvent (fluorine atoms in light blue and oxygen atoms in red) in a cubic cell with a size of 50 Å, with the secondary structure (shown in the inset) in the initial optimized geometry (right) with the distribution of the ψ torsional angles. (For interpretation of the references to color in this figure legend, the reader is referred to the web version of this article.)

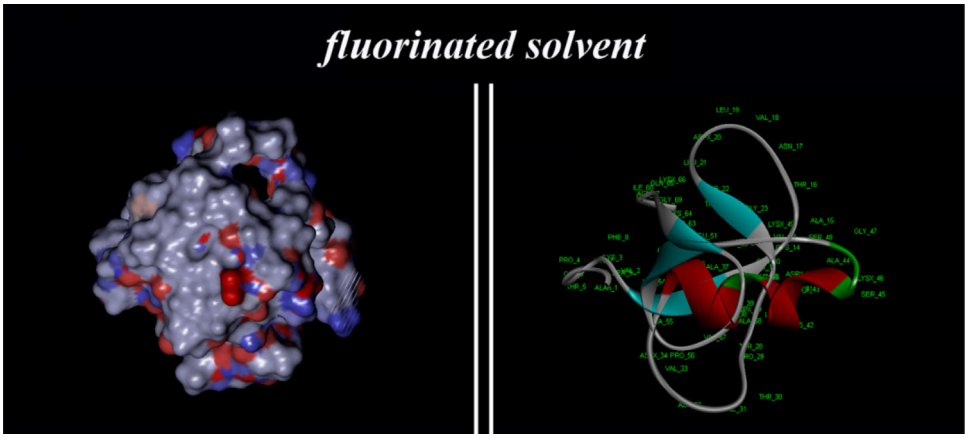

Fig. 8. The surface accessible to a spherical probe having the radius of 1.4 Å of the HFBII in the fluorinated solvent in the initial optimized geometry, viewed from the hydrophobic side (left). A small cavity through the protein is clearly seen in the upper part of the protein. The secondary structure and the labeled aminoacids are reported (right).

water, where a first and a second hydration shell can be detected. Taken together, these results suggest that in this fluorinated solvent the hydrophobic patch assumes its preferred intramolecular conformation, whereas in water it is more compact so as to minimize its interaction with the hydrophilic solvent, as it could be expected.

4. Conclusions

In summary, comparing experimental data and atomistic simulation results, the HFBII protein is, in general, a very stable protein thanks also to its disulphide bridges present in the protein core. Thus, the general shape of the protein calculated in water and at the water/*vacuum* interface is basically the same without any indication of overall denaturation changing the protein envelope. Moreover, HFBII, studied for the first time at the atomistic level in this work in a strongly hydrophobic fluorinated environment, shows only minor local changes in the hydrophobic patch with the formation of a small opening through the protein. Additionally, the atomistic MD simulations, which can describe the changes in the overall shape and in the secondary structure of a protein as well as the global motion involving the molecular translation and rotation in the specific solvent, show that in water HFBII migrates to the water/*vacuum* interface and exposes to *vacuum* its hydrophobic side, comprising amino acids with hydrophobic side chains such as leucine and isoleucine. At the same time, the protein better orients the hydrophilic amino acids towards the water molecules to optimize the intermolecular hydrogen bonds. Finally, in the fluorinated environment HFBII interacts with the hydrophobic solvent by slightly increasing the exposed hydrophobic surface and possibly forming also a small opening. As a conclusion, the conformation of HFBII and the changes in secondary structure can be described using CD spectra, in particular for the ordered part of the backbone structured in α-helices or β-sheets, and atomistic molecular dynamics simulations, that can also describe the possible changes of more disordered random coil strands of the backbone, thus studying the geometrical properties and the dynamical behavior in different environments. Concerning the simulation results, we note that the root-mean-square distance (RMSD) maps and the pair

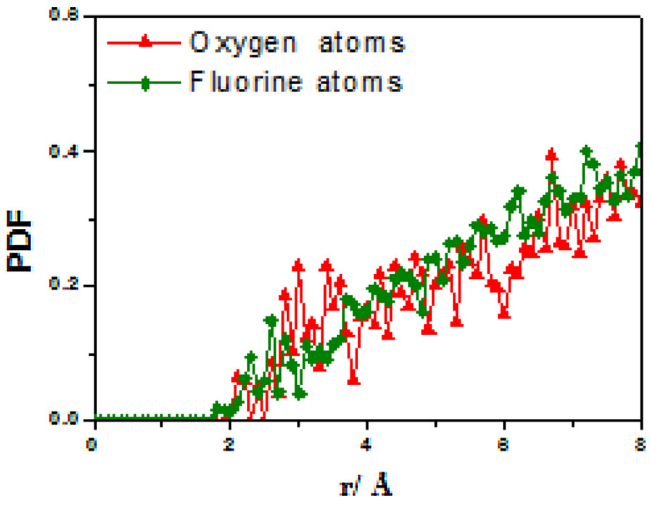

Fig. 9. PDF of the oxygen (in red) and fluorine atoms (in green) around the HFBII protein calculated during the MD run in the fluorinated solvent. (For interpretation of the references to color in this figure legend, the reader is referred to the web version of this article.)

distribution functions (PDF) are most useful tools to respectively describe the conformational changes of the protein, in addition to the Ramachandran maps, and the solvent distribution around it at room temperature, thus possibly helping to understand solvation effects.

We finally stress that a detailed description of the protein conformation and its flexibility in different conditions is a first step but also a pre-requisite to study in future work the self-assembly process of hydrophobins forming dimers or tetramers as a function of the solvent and/or the concentration, as well as their adhesion to various surfaces [24].

Acknowledgments

The authors would like to thank Dr. Géza R. Szilvay, Dr. Arja Paananen and Riitta Suihkonen (VTT-Technical Research Centre of Finland Ltd.) for helpful discussions and protein expression and purification. The authors also gratefully acknowledge the financial support from MIUR—FIRB Futuro in Ricerca 2008 (RBFR08XH0H) and PRIN 2010–2011 (2010PFLRJR_005), and from the Academy of Finland (#276537 and #260565).

Appendix A. Supplementary data

Supplementary data associated with this article can be found, in the online version, at http://dx.doi.org/10.1016/j.jmgm.2015.11.006.

References

[1] M.B. Linder, Hydrophobins: proteins that self assemble at interfaces, Curr. Opin. Colloid Interface Sci. 14 (2009) 356–363.
[2] H.J. Hektor, K. Scholtmeijer, Hydrophobins: proteins with potential, Curr. Opin. Biotechnol. 16 (2005) 434–439.
[3] J. Hakanpää, M. Linder, A. Popov, A. Schmidt, J. Rouvinen, Hydrophobin HFBII in detail: ultrahigh-resolution structure at 0.75 Å, Acta Crystallogr. Sect. D: Biol. Crystallogr. 62 (2006) 356–367.
[4] H.A.B. Wösten, K. Scholtmeijer, Applications of hydrophobins: current state and perspectives, Appl. Microbiol. Biotechnol. 99 (2015) 1587–1597.
[5] J. Hakanpää, G.R. Szilvay, H. Kaljunen, M. Maksimainen, M. Linder, J. Rouvinen, Two crystal structures of *Trichoderma reesei* hydrophobin HFBI—the structure of a protein amphiphile with and without detergent interaction, Prot. Sci. 15 (2006) 2129–2140.
[6] A.R. Cox, D.L. Aldred, A.B. Russel, Exceptional stability of food foams using class II hydrophobin HFBII, Food Hydrocoll. 23 (2009) 366–376.
[7] F. Tchuenbou-Magaia, I. Norton, P. Cox, Hydrophobins stabilised air-filled emulsions for the food industry, Food Hydrocoll. 23 (2009) 1877–1885.
[8] M. Janssen, M. van Leeuwen, K. Scholtmeijer, T. van Kooten, L. Dijklhuizen, H. Wösten, Coating with genetic engineered hydrophobin promotes growth of fibroblasts on a hydrophobic solid, Biomaterials 23 (2002) 4847–4854.
[9] P. Laaksonen, A. Walther, J.M. Malho, M. Kainlauri, O. Ikkala, M.B. Linder, Genetic engineering of biomimetic nano-composites: diblock proteins, graphene and nanofibrillated cellulose, Angew. Chem. Int. Ed. 50 (2011) 8688–8691.
[10] R. Milani, E. Monogioudi, M. Baldrighi, G. Cavallo, V. Arima, L. Marra, A. Zizzari, R. Rinaldi, M. Linder, G. Resnati, P. Metrangolo, Hydrophobin: fluorosurfactant-like properties without fluorine, Soft Matter 9 (2013) 6505–6514.
[11] A. Schulz, B.M. Liebeck, D. John, A. Heiss, T. Subkowski, A. Böker, Protein–mineral hybrid capsules from emulsions stabilized with an amphiphilic protein, J. Mater. Chem. 21 (2011) 9731–9736.
[12] C. Pigliacelli, A. D'Elicio, R. Milani, G. Terraneo, G. Resnati, F. Baldelli Bombelli, P. Metrangolo, Hydrophobin-stabilized dispersions of PVDF nanoparticles in water, J. Fluorine Chem. 177 (2015) 62–69.
[13] R. Milani, L. Pirrie, L. Gazzera, A. Paananen, M. Baldrighi, E. Monogioudi, G. Cavallo, M. Linder, G. Resnati, P. Metrangolo, A synthetically modified hydrophobin showing enhanced fluorous affinity, J. Colloid Interface Sci. 448 (2015) 140–147.
[14] F. Ganazzoli, G. Raffaini, Computer simulation of polypeptide adsorption on model biomaterials, Phys. Chem. Chem. Phys. 7 (2005) 3651–3663.
[15] G. Raffaini, F. Ganazzoli, Understanding the performance of biomaterials through molecular modeling: crossing the bridge between their intrinsic properties and the surface adsorption of proteins, Macromol. Biosci. 7 (2007) 552–566.
[16] G. Raffaini, F. Ganazzoli, Molecular modelling of protein adsorption on the surface of titanium dioxide polymorphs, Phil. Trans. R. Soc. A 370 (2012) 1444–1462.
[17] G. Raffaini, F. Ganazzoli, Surface topography effects in protein adsorption on nanostructured carbon allotropes, Langmuir 29 (2013) 4883–4893.
[18] G. Raffaini, F. Ganazzoli, Surface hydration of polymeric (bio) materials: a molecular dynamics simulation study, J. Biomed. Mater. Res. 92A (2010) 1382–1391.
[19] D.L. Cheung, Molecular simulation of hydrophobin adsorption at an oil-water interface, Langmuir 28 (2012) 8730–8873.
[20] S.R. Euston, Molecular simulation of adsorption of hydrophobin HFBI to the air–water, DPPC–water and decane–water interfaces, Food Hydrocoll. 42 (2014) 66–74.
[21] M. Linder, K. Selber, T. Nakari-Setälä, M. Qiao, M. Kula, M. Penttilä, The hydrophobins HFBI and HFBII from *Trichoderma reesei* showing efficient interactions with nonionic surfactants in aqueous two-phase systems, Biomacromolecules 2 (2001) 511–517.
[22] InsightII/Discover, Materials Studio, Discovery Studio distributed by Accelrys Inc., San Diego, CA. See http://www.accelrys.com.
[23] S. Askolin, M. Linder, K. Scholtmeijer, M. Tenkanen, M. Penttila, M.L. de Vocht, H.A.B. Wosten, Interaction and comparison of a class I hydrophobin from schizophyllum commune and class II hydrophobins from *Trichoderma reesei*, Biomacromolecules 7 (2006) 1295–1301.
[24] L. Gazzera, C. Corti, L. Pirrie, A. Paananen, A. Monfredini, G. Cavallo, S. Bettini, G. Giancane, L. Valli, M.B. Linder, G. Resnati, R. Milani, P. Metrangolo, Hydrophobin as a nanolayer primer that enables the oleophobic coating of poorly reactive polymer surfaces, Adv. Mater. Interfaces (2015) 1500170-1–1500170-8.